Reconstructing the 20th century high-resolution climate of the southeastern United States

Steven M. DiNapoli[1] and Vasubandhu Misra[1,2]

Received 15 June 2012; revised 23 August 2012; accepted 31 August 2012; published 9 October 2012.

[1] We dynamically downscale the 20th Century Reanalysis (20CR) to a 10-km grid resolution from 1901 to 2008 over the southeastern United States and the Gulf of Mexico using the Regional Spectral Model. The downscaled data set, which we call the **F**lorida Climate Institute-Florida State University Land-Atmosphere Reanalysis for the **S**outheastern United States at 10-km resolution (FLAReS1.0), will facilitate the study of the effects of low-frequency climate variability and major historical climate events on local hydrology and agriculture. To determine the suitability of the FLAReS1.0 downscaled data set for any subsequent applied climate studies, we compare the annual, seasonal, and diurnal variability of temperature and precipitation in the model to various observation data sets. In addition, we examine the model's depiction of several meteorological phenomena that affect the climate of the region, including extreme cold waves, summer sea breezes and associated convective activity, tropical cyclone landfalls, and midlatitude frontal systems. Our results show that temperature and precipitation variability are well-represented by FLAReS1.0 on most time scales, although systematic biases do exist in the data. FLAReS1.0 accurately portrays some of the major weather phenomena in the region, but the severity of extreme weather events is generally underestimated. The high resolution of FLAReS1.0 makes it more suitable for local climate studies than the coarser 20CR.

Citation: DiNapoli, S. M., and V. Misra (2012), Reconstructing the 20th century high-resolution climate of the southeastern United States, *J. Geophys. Res.*, *117*, D19113, doi:10.1029/2012JD018303.

1. Introduction

[2] There is presently a high demand among climate scientists for long-term reanalyses of atmospheric state variables [*Bengtsson et al.*, 2007]. These long-term reanalyses provide scientists with several decades of atmospheric data assimilated on a uniform grid, using state of the art data analysis techniques, which eases climate analysis. Several such reanalyses have been developed since the mid-1990s [*Kalnay et al.*, 1996; *Kanamitsu et al.*, 2002; *Uppala et al.*, 2005; *Onogi et al.*, 2007; *Saha et al.*, 2010; *Dee et al.*, 2011; *Rienecker et al.*, 2011]. But the 20th Century Reanalysis (20CR) [*Compo et al.*, 2011] is unique because it goes back to the late 19th century, which allows climate scientists to study the impacts of major climate events prior to the widespread use of upper-air observations. The larger data set also allows scientists to study long-term trends in the climate record. Furthermore 20CR is also unique in using consistently only one type of observed information to assimilate, namely, the synoptic observations of surface pressure. This avoids introduction of any artificial variability in the reanalysis from changing observation systems, thus making 20CR ideal in some ways for climate diagnostic analysis. 20CR has 2° grid spacing and a 6-hourly time interval, which may be sufficient for global-scale analysis, but is too coarse for use in regional climate studies because of the inability to resolve mesoscale features.

[3] In this paper, we dynamically downscale the 20CR to create a 10-km data set over the southeastern United States. The dynamical downscaling method involves integrating a regional scale model using the global reanalysis data as boundary conditions with scale selective bias correction [*Kanamaru and Kanamitsu*, 2007a]. Many studies have shown that some form of nudging in the interior of the regional domain at the largest wavelengths toward the driving large scale field is necessary to reduce the climate drift of the regional climate model [*von Storch et al.*, 2000; *Castro et al.*, 2005]. This nudging in RSM takes the form of scale selective bias correction, which results in a much superior simulation of the regional climate [*Kanamitsu et al.*, 2010]. *von Storch et al.* [2000] and *Kanamitsu and Kanamaru* [2007] claim that when a global reanalysis is downscaled using a regional climate model with some form of nudging in the interior of the domain, the resulting output from the regional model has qualities comparable to that of a regional reanalysis obtained

[1]Center for Ocean-Atmospheric Prediction Studies, Florida State University, Tallahassee, Florida, USA.
[2]Department of Earth, Ocean and Atmospheric Science, Florida State University, Tallahassee, Florida, USA.

Corresponding author: V. Misra, Center for Ocean-Atmospheric Prediction Studies, Florida State University, 2035 E. Paul Dirac Dr., 200 RM Johnson Bldg., Tallahassee, FL 32306-2840, USA. (vmisra@fsu.edu)

0148-0227/12/2012JD018303

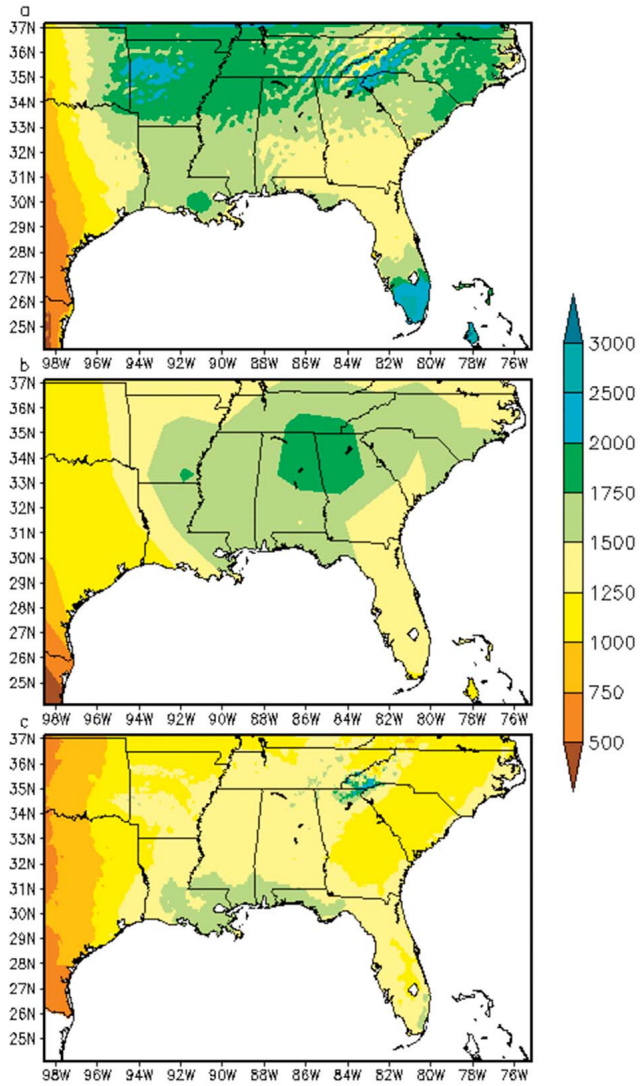

Figure 1. Average annual accumulated precipitation in mm from (a) FLAReS1.0, (b) 20CR, and (c) PRISM.

from a traditional data assimilation approach. The regional model we use for downscaling is the Regional Spectral Model (RSM), which was developed at the National Centers for Environmental Prediction (NCEP) [*Juang and Kanamitsu*, 1994] with the most recent updates to it described in *Kanamitsu et al.* [2010] and references therein.

[4] A similar project of dynamical downscaling the NCEP-National Center for Atmospheric Research (NCAR) Reanalysis to a 10-km grid resolution over the state of California using the RSM is described in *Kanamitsu and Kanamaru* [2007]. Their study shows that the downscaled reanalysis (CaRD10) is able to accurately simulate local mesoscale events and wind patterns. Although CaRD10 displays bias in the temperature and precipitation data, the trends and the variability are reasonably accurate across most timescales. In addition, the CaRD10 data is in reasonable agreement with the North American Regional Reanalysis [*Mesinger et al.*, 2006], and is capable of showing more detail due to its higher resolution [*Kanamaru and Kanamitsu*, 2007b]. The success of CaRD10 was one of the primary motivations for the Center for Ocean-Atmospheric Prediction Studies (**C**OAPS) **L**and-**A**tmosphere **R**egional **R**eanalysis for the **S**outheast at **10**-km resolution (CLARReS10) [*Stefanova et al.*, 2012]. CLARReS10 used the RSM to dynamically downscale both the NCEP-DOE Reanalysis II and the European Center for Medium-Range Weather Forecasts (ECMWF) ERA40 reanalyses over the southeastern United States. CLARReS10 shows a significant improvement in the representation of the diurnal and seasonal cycles of rainfall over the global reanalyses, especially over the state of Florida, which again is a result of the improved resolution of the downscaled data and the relatively high fidelity of the RSM [*Stefanova et al.*, 2012; *Misra et al.*, 2011].

[5] Our study is similar to the CLARReS10 project, but it downscales the 20CR for the years 1901 through 2008. Our data set, which we call the Florida Climate Institute-Florida State University Land-Atmosphere Reanalysis for the **S**outheastern United States at 10-km Resolution version 1.0 (FLAReS1.0), allows for the study of the effects of multi-decadal climate variability on local hydrology and agriculture, and it also allows for the investigation of major climate events in the first half of the 20th century, which is otherwise not possible with CLARReS10. In addition, FLAReS1.0 has a larger domain than CLARReS10, encompassing the entire region surrounding the Gulf of Mexico, and it utilizes an updated version of the RSM (with updates primarily in the scale selective bias correction [*Kanamitsu et al.*, 2010]). In this paper, we compare the downscaled reanalysis data against several observation data sets to determine how well FLAReS1.0 depicts regional climate processes. We also contrast FLAReS1.0 with CLARReS10.

2. Data and Methods

2.1. RSM Description and Model Configuration

[6] The RSM is a primitive equation model that uses boundary conditions from the global reanalysis, in this case 6-hourly analyses from the 20CR. A scale-selective bias correction (SSBC) scheme spectrally nudges the perturbations of the RSM from the 20CR in the interior of the domain, which prevents unrealistic regional climate drift of the RSM [*von Storch et al.*, 2000; *Kanamaru and Kanamitsu*, 2007a]. In addition, the SSBC scheme reduces the sensitivity of the RSM to the size and location of the regional domain [*Kanamaru and Kanamitsu*, 2007a]. In the version used for generating FLAReS1.0, RSM nudges the rotational component of the wind toward the C20R for wavelengths greater than or equal to 500 km and sets the area average temperature perturbation of the regional domain to zero as part of its scale selective bias correction following *Kanamitsu et al.* [2010]. The model domain extends from approximately 16.2°N to 37.8°N and from 99.4°W to 74.4°W, which encompasses the southeastern United States, the Gulf of Mexico, and the northern Caribbean Sea. The physics and parameterization schemes are unchanged from the CLARReS10 runs [*Stefanova et al.*, 2012]. Specifically, we use the simplified Arakawa-Schubert deep convection scheme [*Hong and Pan*, 1998], the shallow convection scheme described by *Tiedtke* [1983], the cloud parameterization scheme from *Slingo* [1987], and the NOAH land surface scheme [*Ek et al.*, 2003]. We prescribe daily sea

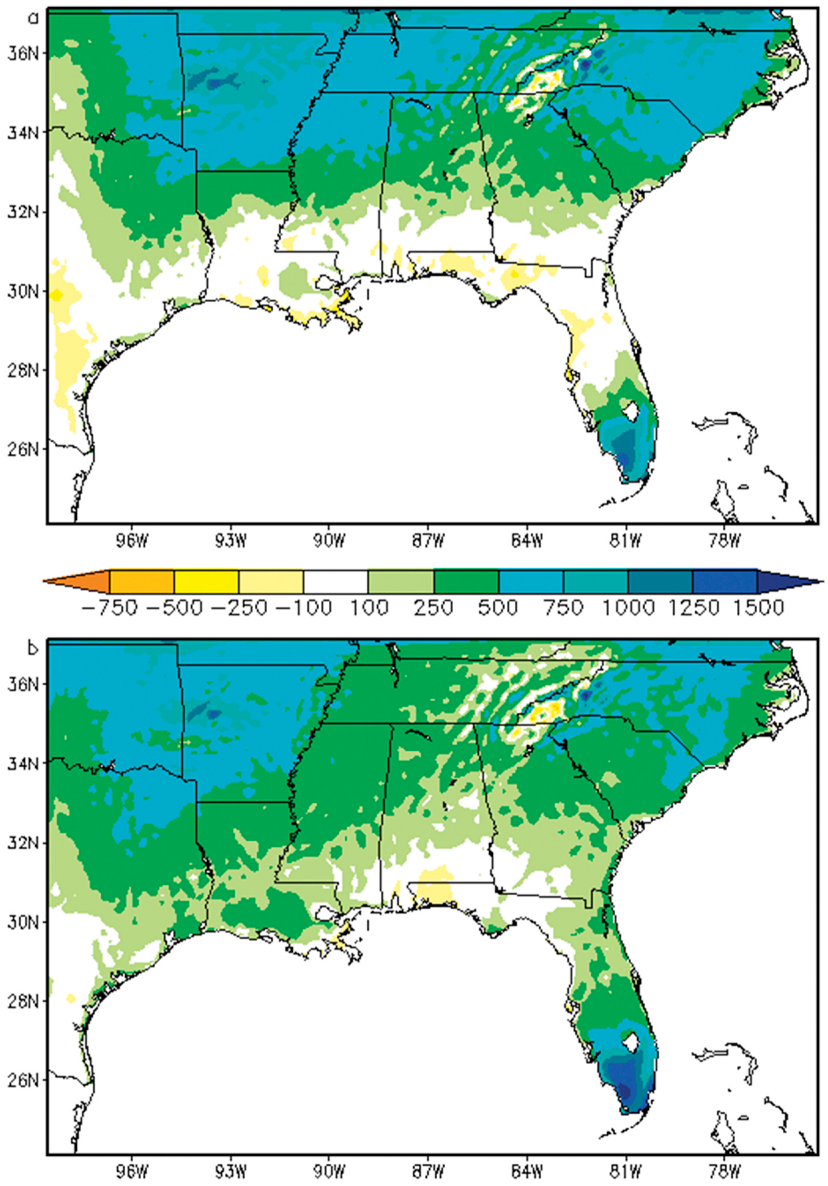

Figure 2. Average annual precipitation bias (mm) of FLAReS1.0 computed relative to and PRISM for the period (a) 1903–1949 and (b) 1950–1999.

surface temperatures from the UK Met Office HADISST [*Rayner et al.*, 2003], which is consistent with 20CR forcing.

[7] The RSM is run from 1901 through 2008, but in order to reduce the computing time, we parallelize the process by running the RSM simultaneously for three subset periods (streams) with an overlapping period of 5 years to account for any spin-up issues. These subsets contain the years 1901–1939, 1935–1974, and 1970–2008. At the end of the five-year overlap period, the subsets were found to be extremely well correlated for most variables, with correlation coefficients greater than 0.95. Precipitation was a notable exception due to the often chaotic nature of convective storms. To minimize discontinuities at the transition period, we merge the data sets from the three streams at times when there is little to no precipitation in the model domain during this 5 year overlap period.

2.2. Verification Data

[8] Our verification of the FLAReS1.0 downscaled reanalysis focuses primarily on precipitation and temperature variability as they hold lot of significance for any ensuing application studies. Moreover the long-term observed analysis of temperature and precipitation are among the most easily accessible in the climatological database [e.g., *Mitchell and Jones*, 2005; *Daly et al.*, 1994]. To validate annual means and variability on seasonal to interannual time scales, we use monthly temperature data from the Climate Research Unit version 3.1 (CRU) time series [*Mitchell and Jones*, 2005]. This

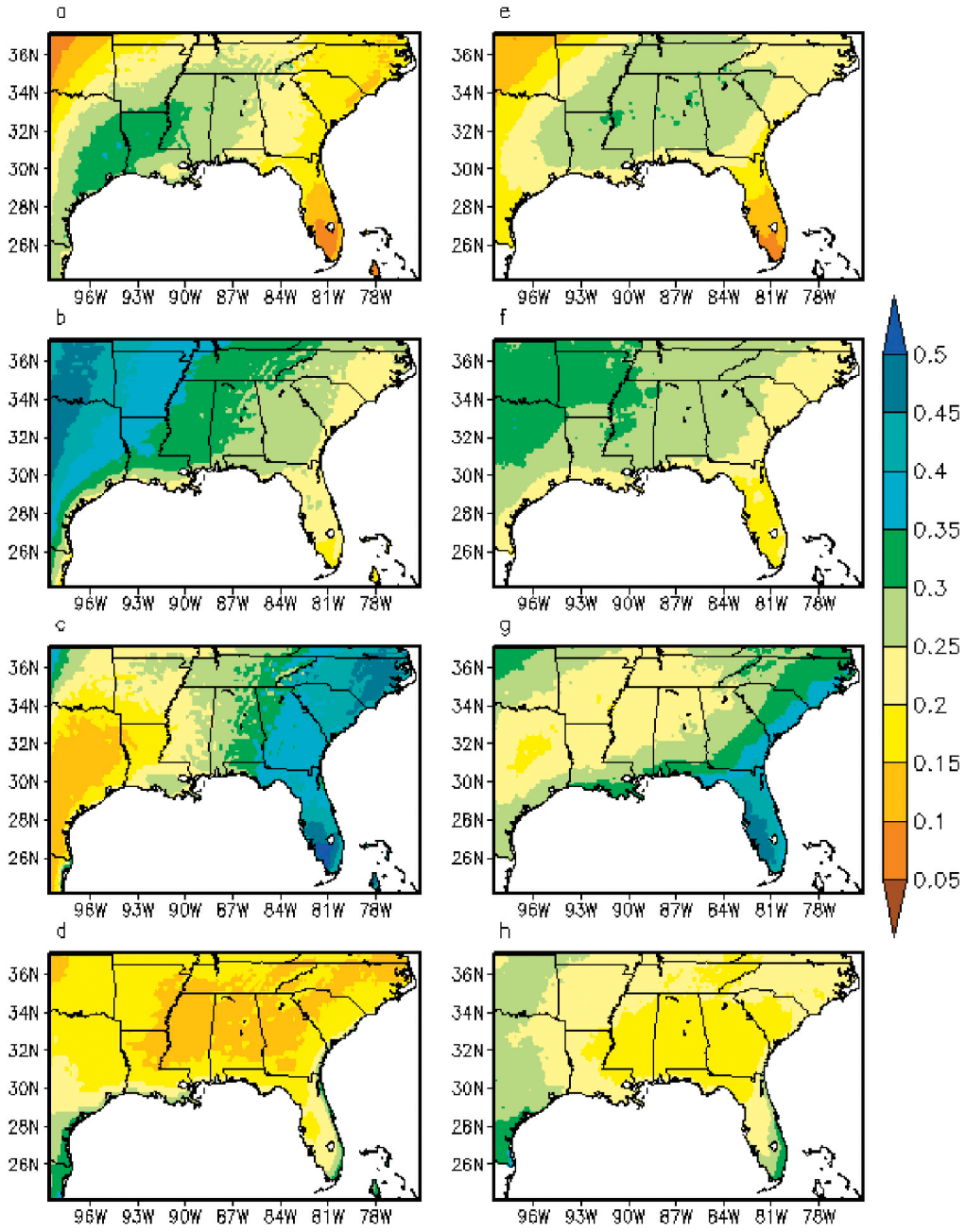

Figure 3. Fraction of the annual total precipitation falling in the months of (a) December–February (DJF), (b) March–May (MAM), (c) June–August (JJA), and (d) September–November (SON) from FLAReS1.0. (e–h) The same as Figures 3a–3d but from PRISM.

data set covers all land areas within the FLAReS1.0 domain at 0.5° grid spacing, and is available for the entire 20th century. For precipitation, we use the Parameter-elevation Regressions on Independent Slopes Model (PRISM) [*Daly et al.*, 1994] monthly precipitation data, which only covers the continental United States, but has 4-km grid spacing. The PRISM data set also covers the entire 20th century.

[9] To validate day-to-day precipitation variability, we utilize the National Oceanic and Atmospheric Administration (NOAA) Climate Prediction Center (CPC) Daily U.S. Unified Precipitation at 0.25° resolution [*Higgins et al.*, 1996]. This data set is available from 1948 to 2006 over the continental United States. For daily temperature observations, we use data from several observing stations in the southeastern United States, which are obtained from the National Climatic Data Center in Asheville, North Carolina. These stations include Atlanta, GA; Charleston, SC; Jackson, MS; Jacksonville, FL; Montgomery, AL; New Orleans, LA; Tallahassee, FL; Tampa, FL; and Miami, FL. We also utilize hourly precipitation data from the NCEP/Environmental Modeling Center (EMC) U.S.

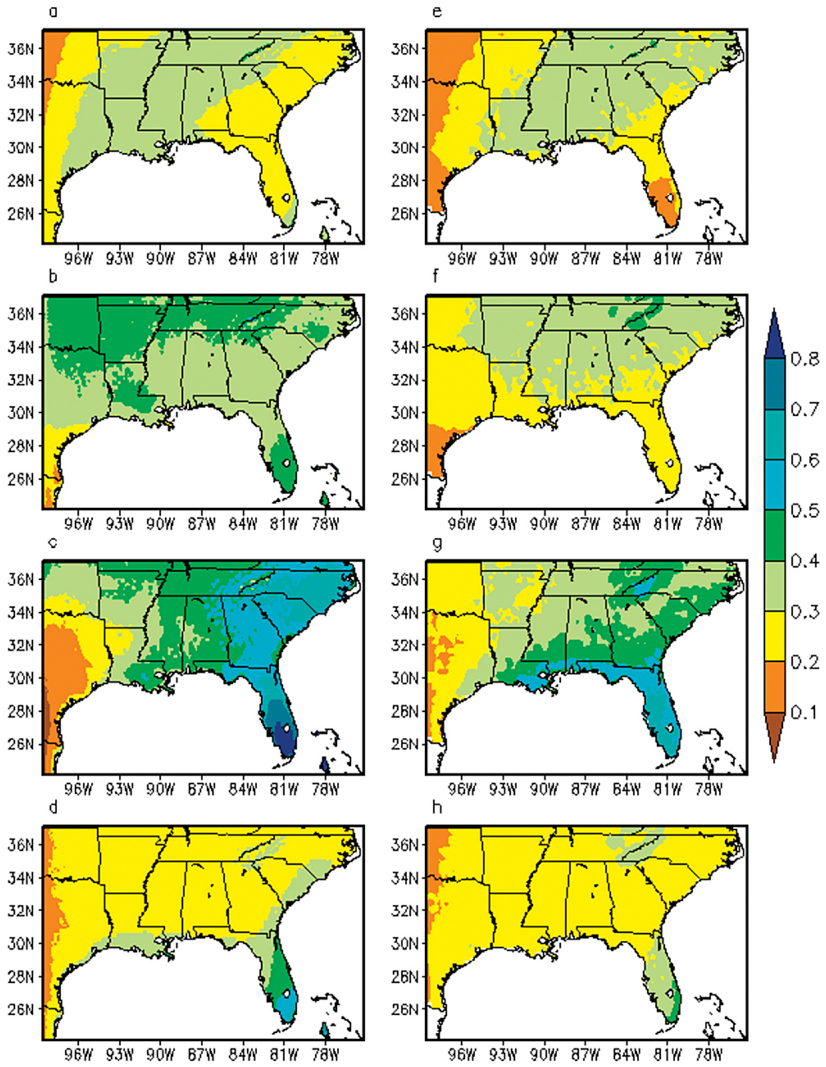

Figure 4. Fraction of days with at least 1 mm of precipitation in (a) DJF, (b) MAM, (c) JJA, and (d) SON from FLAReS1.0. (e–h) The same as Figures 4a–4d but from the CPC Daily U.S. Unified Precipitation data set.

gridded precipitation analysis at 4 km [*Lin and Mitchell*, 2005] to verify diurnal variability. This data is derived from rain gauges and radar estimates, and is only available from 2002 onwards.

3. Results

3.1. Precipitation

[10] We begin our verification of the FLAReS1.0 data by calculating the average annual precipitation and comparing it to the 20CR and PRISM data (Figure 1). We note a large wet bias in FLAReS1.0 over much of the northern part of the domain, stretching from eastern Oklahoma to the Carolinas. This bias is also present in the 20CR, but has a lesser magnitude. In addition, the southern tip of Florida has an extremely wet bias in FLAReS1.0, which is completely absent in 20CR. The CLARReS-ERA downscaled reanalysis [*Stefanova et al.*, 2012] has similar biases in North Carolina and South Florida, indicating the presence of a bias within the RSM. Using the CRU precipitation data set instead of PRISM yields similar results (not shown). Despite these biases, FLAReS1.0 does well in projecting several spatial precipitation patterns, including the local precipitation maximum over the north central Gulf Coast and the drying trend toward central and western Texas. We also calculate the average bias between FLAReS1.0 and PRISM before and after 1950 (Figure 2). The bias patterns are similar during these two periods, but they are slightly larger north of 32°N in the pre-1950 period, likely the result of the parent 20CR having fewer observations. However, it is reassuring to note that the fidelity of the mean state of the downscaled reanalysis is comparable in the two epochs.

[11] We next examine the seasonal cycle of precipitation in FLAReS1.0, and whether it contributes to any of the biases examined in the annual mean. Figure 3 shows the fraction of climatological average seasonal (3-month)

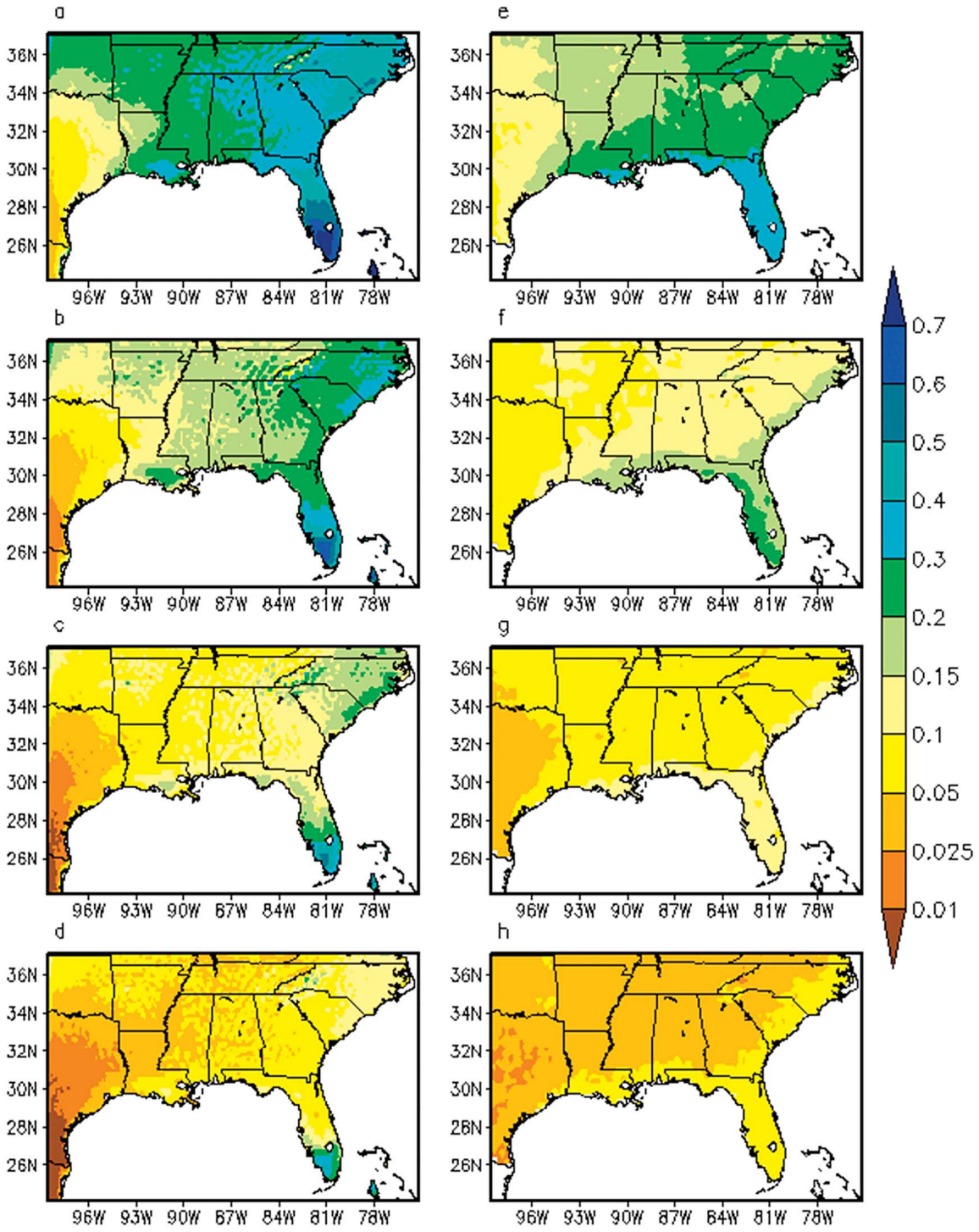

Figure 5. Fraction of days in JJA with at least (a) 5 mm, (b) 10 mm, (c) 15 mm, and (d) 20 mm of precipitation from FLAReS1.0. (e–h) The same as Figures 5a–5d but from the CPC Daily U.S. Unified Precipitation data set.

precipitation divided by the average annual total precipitation in each season of the year for both FLAReS1.0 and the PRISM data. Over most of the domain, the seasonal cycle is very well represented by FLAReS1.0. The summer (winter) maximum (minimum) in precipitation over Florida is clearly reflected in the model. The summer maximum extends northward toward Georgia and the Carolinas as in the observations, but FLAReS1.0 overestimates it by as much as

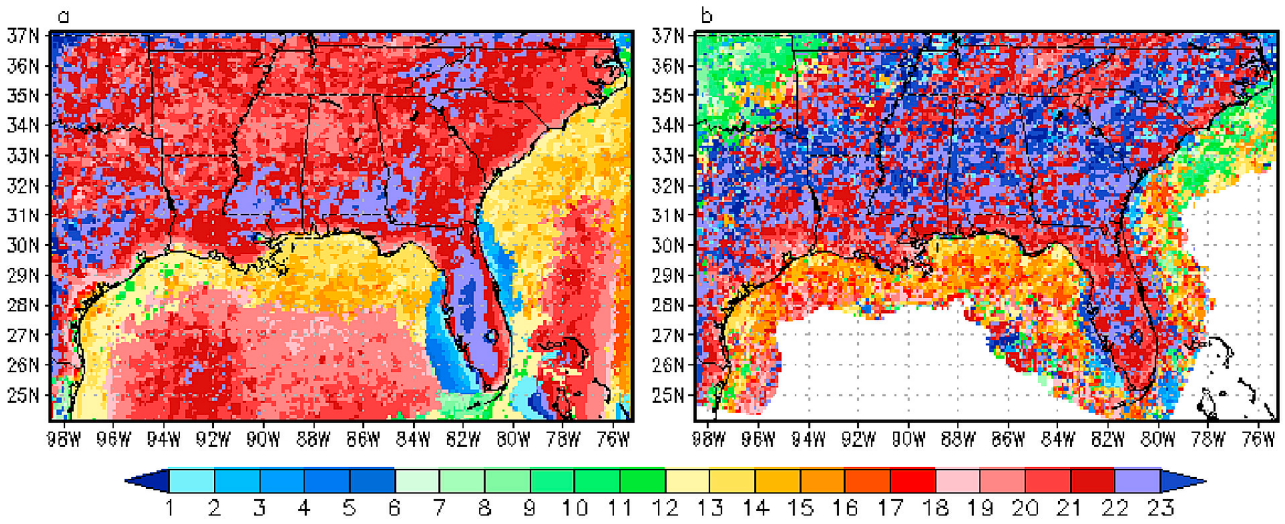

Figure 6. The timing (UTC) of the climatological diurnal precipitation maximum in JJA from (a) FLAReS1.0 and (b) the NCEP/EMC hourly precipitation data.

15%. Similarly, a spring maximum in precipitation occurs in Texas, Oklahoma, and Arkansas like the observations; this is also overestimated in FLAReS1.0 with a corresponding erroneous reduction in the fraction of precipitation in the summer and fall seasons over these areas. Elsewhere, the relative fractions of precipitation in each season are generally reasonable in FLAReS1.0 to within 5–10%. We therefore conclude that in the northern part of the domain, increased rainfall in the spring and summer seasons contributes toward the bias in the annual mean; however, in Florida, the seasonal cycle is well-represented and therefore is not the primary cause of the annual mean bias.

[12] To determine the cause of the FLAReS1.0 precipitation bias over Florida, we check to see whether the bias is a result of increased number of rainy days or increased frequency of heavy precipitation events. We begin by calculating the fraction of rainy days exceeding 1 mm of rainfall for each season of the year (Figure 4) for FLAReS1.0 and the CPC daily U.S. unified precipitation data set. From this figure, we see that the percentage of rainy days in southern Florida is at least 10–20% higher in FLAReS1.0 than in the observations in every season of the year. The precipitation frequency is also too high in the spring and summer seasons over the northern part of the domain, but elsewhere it is well represented. In addition, we calculate the percentage of days with greater than 5, 10, 15, and 20 mm of precipitation in the summer months (Figure 5). South Florida is biased high in FLAReS1.0 at all four thresholds, indicating that the precipitation excess there is caused by both an increase in rainy days and an increase in heavy precipitation events. We therefore believe that the convective schemes used in the RSM are triggering precipitation in South Florida too frequently, and the precipitation generated in the model is too heavy in this region. In the Carolinas, there is also an increase in heavy precipitation events, but farther west the biases are reduced for the higher precipitation thresholds, indicating that the seasonal excess there is caused by an increase in the frequency of light precipitation events.

[13] The majority of summer rainfall in the southeastern United States is convective in nature, and is favored to occur during the peak heating hours of the day. In addition, local sea breeze circulations can create a strong diurnal precipitation signal near the coasts [*Byers and Rodebush*, 1948]. To make sure these diurnal signals are accurately represented in FLAReS1.0, we calculate the climatological hour of maximum precipitation during the summer months for both FLAReS1.0 and the NCEP/EMC hourly precipitation data (Figure 6). It may be noted that the NCEP/EMC precipitation data is only available from 2002 onward, which restricts us to compare the climatology of the diurnal variability of precipitation. Near the Gulf Coast region, the diurnal maximum in the FLAReS1.0 data occurs as early as 1900 UTC (3:00 P.M. EDT) near the coast, and as late as 0000 UTC (8:00 P.M. EDT) farther inland. This is generally in good agreement with the NCEP/EMC data and CLARReS-ERA [*Stefanova et al.*, 2012] (not shown), and the inland progression of the sea breeze circulation with time is clearly evident in both data sets. Farther north, however, the diurnal maximum occurs several hours earlier in FLAReS1.0 than in the observations. In this area, CLARReS-R2 is much closer to observations than either CLARReS-ERA or FLAReS1.0 (not shown). Figure 7 shows the diurnal precipitation cycle for several point locations. FLAReS1.0 clearly displays the diurnal cycle in all of the cases shown, but Atlanta, Charleston, Montgomery, and to a lesser extent Jackson all have the onset of convection occur earlier in FLAReS1.0 than in the observations. In addition, the peak convective period at these locations lasts several hours in the model, whereas it is much shorter in the observations. The diurnal cycle is much more accurately represented closer to the coastline, particularly in Tallahassee and in Jacksonville, Florida.

3.2. Temperature

[14] The average temperatures for each season of the year over the southeastern United States are shown in Figure 8 for FLAReS1.0, 20CR, and CRU. Generally, both FLAReS1.0

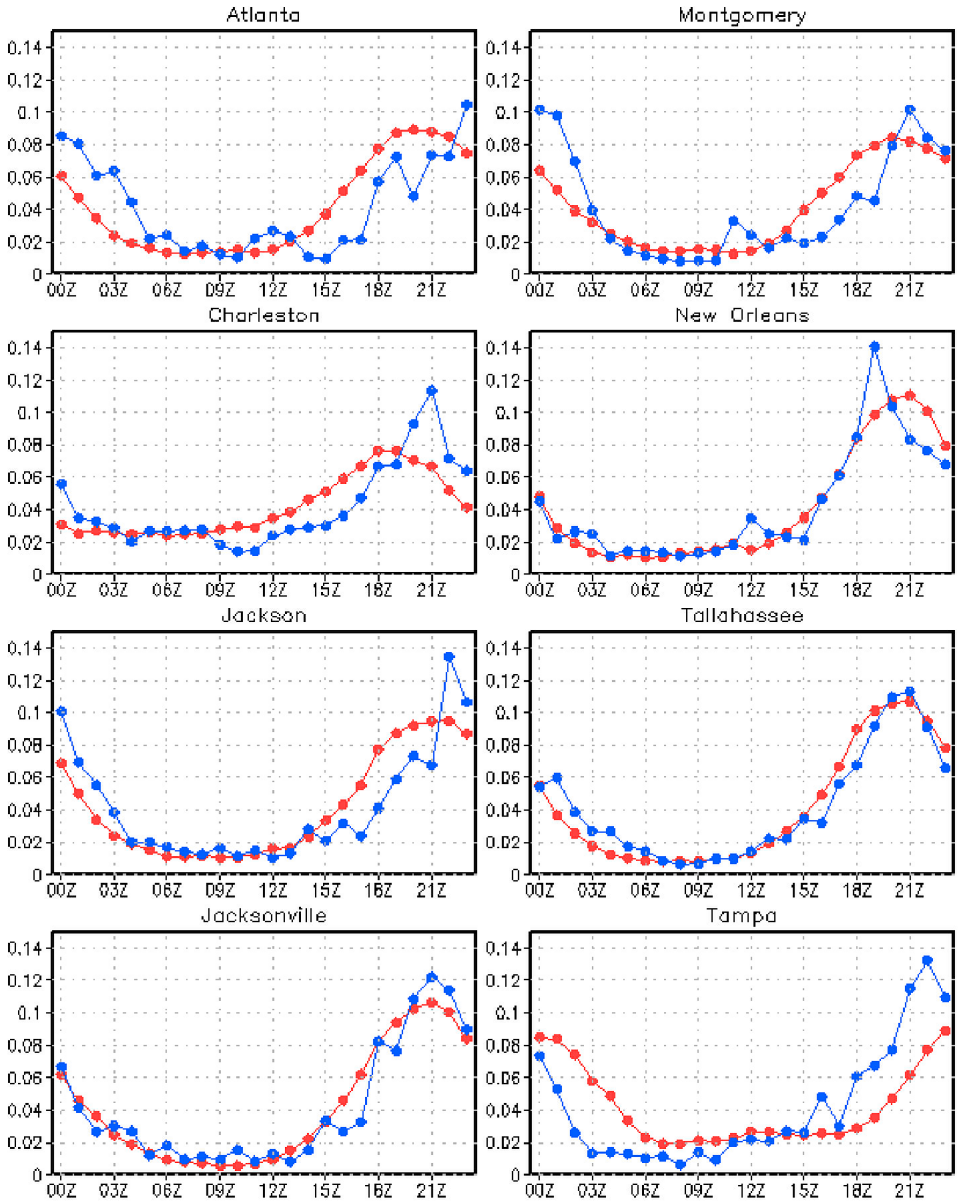

Figure 7. The fraction of JJA precipitation falling at each hour of the day for several major cities from FLAReS1.0 (red) and the NCEP/EMC hourly precipitation data (blue).

and 20CR are in strong agreement with the observations on the seasonal temperature cycle over the vast majority of the region. Calculating model biases relative to the observations (Figure 9) shows that there is a warm bias in FLAReS1.0 over parts of Texas, which persists throughout the year; this bias expands eastward toward Mississippi and Alabama during the summer months. A cold bias exists near the northern edge of the domain in winter and spring, which is also present in 20CR. In addition, both FLAReS1.0 and 20CR have a cold bias over the Carolinas throughout the year. It is clear that some of the biases in 20CR are being propagated into FLAReS1.0; however, other biases in 20CR, such as the extreme warm bias in Florida in the winter months, are removed in FLAReS1.0 as a result of better topographic and land-sea mask resolution.

[15] The occurrence of sub-freezing temperatures in the winter season has a significant impact on agriculture in the southeastern United States, especially in Florida [*Miller and Downton*, 1993; *Downton and Miller*, 1993]. To determine how well FLAReS1.0 simulates freeze events, we compare the number of freezes in the model to the climatological records for several cities in each winter from 1948–49 through 1989–90 (Figure 10). The number of freeze events in a given year is generally well correlated between FLAReS1.0 and the observations; however several biases exist in the time series. The model has a tendency to overestimate the number of freeze events prior to 1972 and to underestimate the number of freezes thereafter. In the observations there is a noticeable upward trend in the number of freezes per year at most locations, but this is not

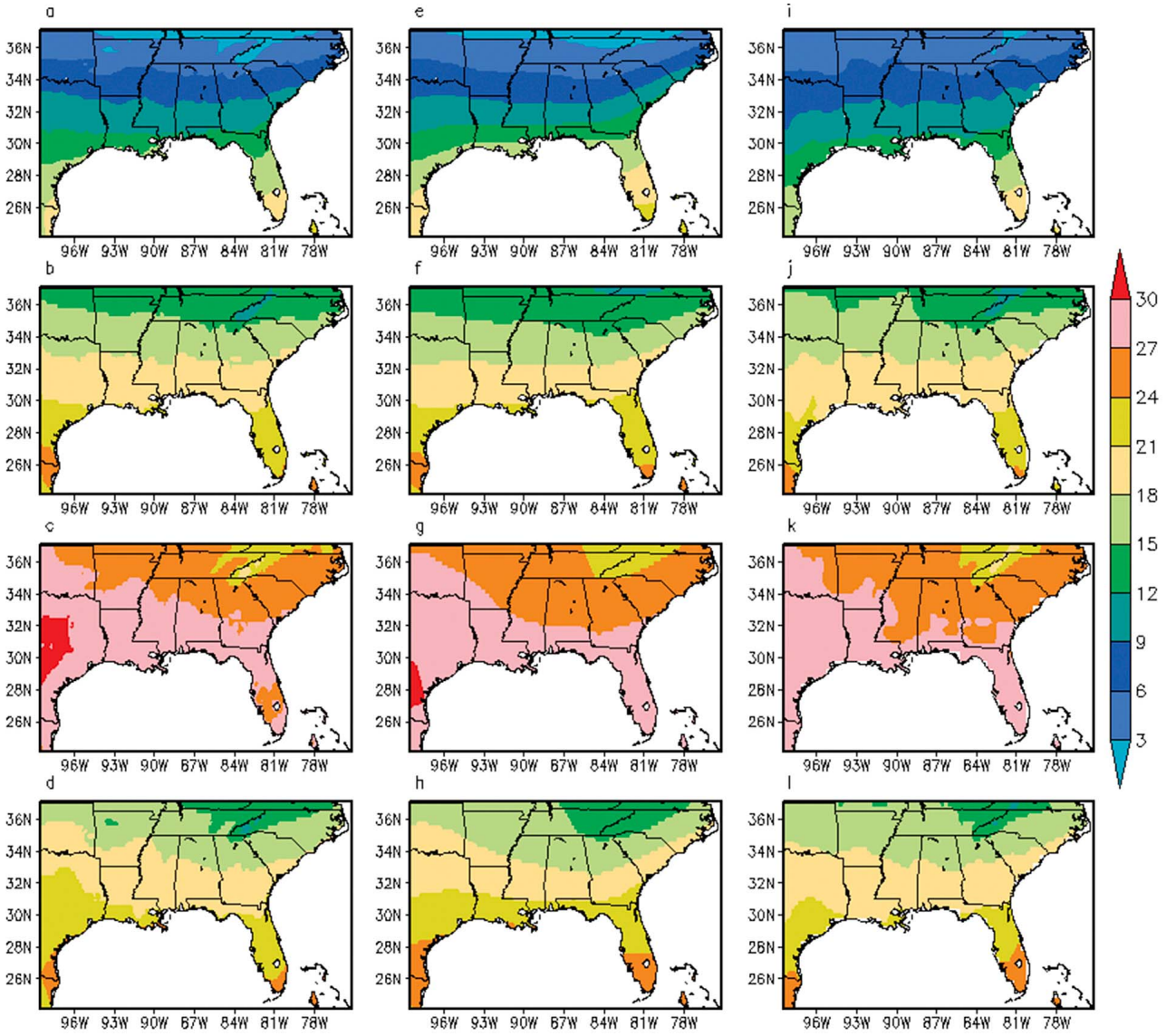

Figure 8. Climatological average seasonal temperature (°C) during (a) DJF, (b) MAM, (c) JJA, and (d) SON from FLAReS1.0. (e–h) The same as Figures 8a–8d but from 20CR. (i–l) The same as Figures 8a–8d but from CRU.

evident in FLAReS1.0. The upward trend in the observations may be caused by changes in land use, which cannot be detected in FLAReS1.0 as it did not adopt a time varying land use. The winters of 1976–77 and 1977–78 were particularly severe, with record numbers of freezes being recorded in several locations. FLAReS1.0 correctly shows an abnormally large number of freezes in those winters, but tends to underestimate the extreme numbers. Miami (not shown) only recorded freezes in January 1977, January 1985, and December 1989. In FLAReS1.0, sub-freezing temperatures only occurred in the January 1977 event over Miami.

3.3. Case Studies

[16] In this subsection we analyze several significant weather events using the FLAReS1.0 data. We begin by studying the model's depiction of the January 1985 cold wave, which was one of the most severe Florida citrus freezes in recent history [*Miller*, 1991]. 500–1000 hPa thickness plots overlaid with 850 hPa wind vectors averaged over 20 Jan. 1985 (Figure 11a) clearly show a sharp thickness gradient with northerly winds in excess of 20 ms^{-1}, indicating the presence of strong cold advection over most of the region. On 21 Jan (Figure 11b), the cold advection moves into Florida, whereas the cold wave is at its peak in the Tennessee Valley and the southern Appalachian Mountains. Florida reaches its minimum thickness values on 22 Jan (Figure 11c), at which point the cold advection begins to weaken substantially. By 23 Jan (Figure 11d), the air mass has begun to moderate, and cold advection has ceased over most of the domain. In Figure 12 we plot the minimum temperature in FLAReS1.0 over the four-day period. FLAReS1.0 accurately shows subfreezing temperatures extending into south Florida, but in general the temperatures are biased too high. Observed minimum temperatures across

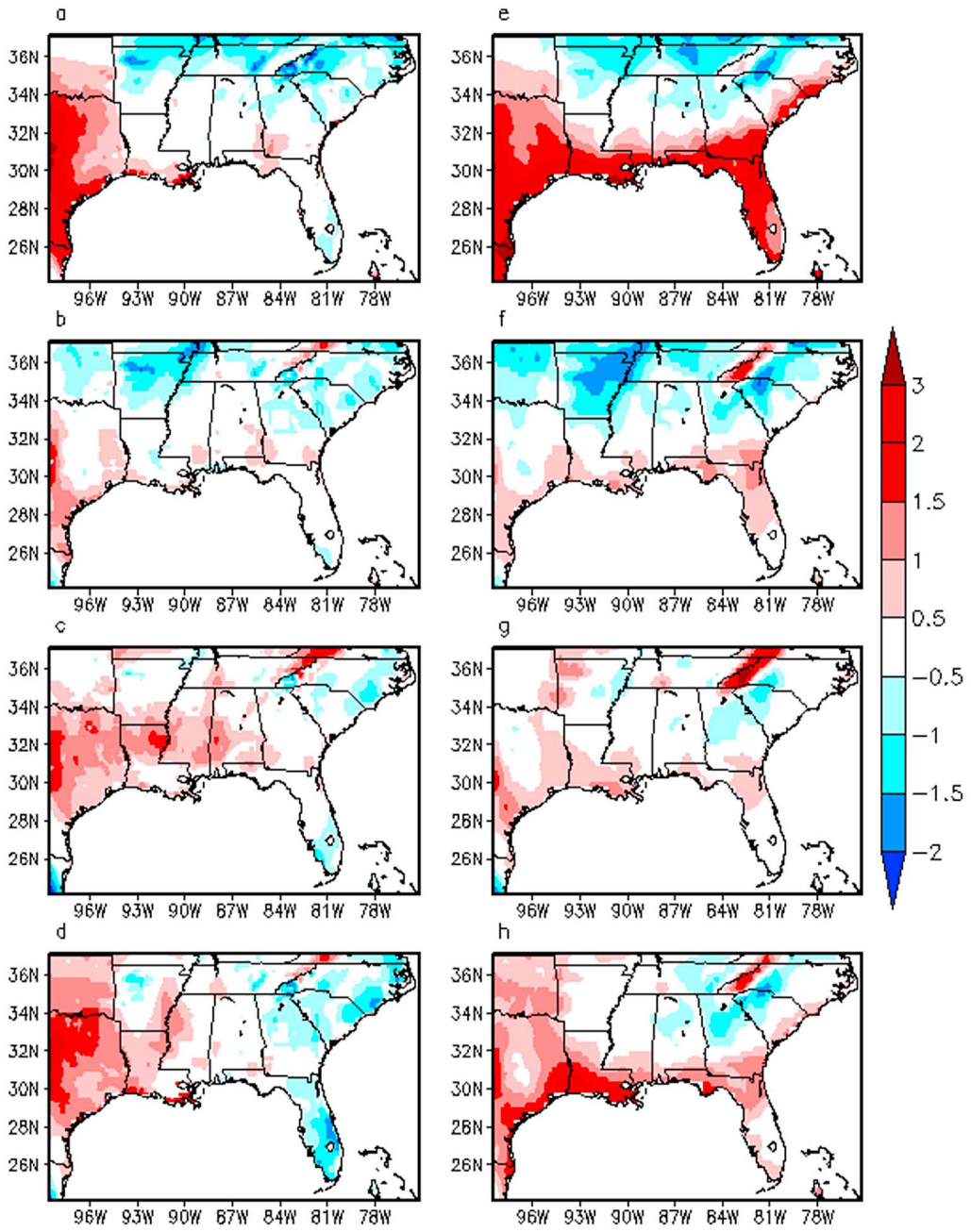

Figure 9. Climatological average seasonal temperature bias (°C) between FLAReS1.0 and CRU during (a) DJF, (b) MAM, (c) JJA, and (d) SON from FLAReS1.0. (e–h) The same as Figures 9a–9d but showing the bias between 20CR and CRU.

the region include −10°C in New Orleans, −22°C in Atlanta, −14°C in Tallahassee, and −6°C in Tampa. We therefore conclude that although FLAReS1.0 clearly shows the synoptic conditions leading up to the cold wave, it underestimates the severity. The CLARReS-ERA and CLARReS-R2 downscaled reanalyses [*Stefanova et al.*, 2012] depict the minimum temperatures with much greater accuracy, likely a result of having more observed data in the driving global reanalyses (not shown).

[17] S. Bastola and V. Misra (Sensitivity of hydrological simulations of southeastern United States watersheds to temporal aggregation of rainfall, submitted to *Journal of Hydrometeorology*, 2012) showed from observations that summer seasonal precipitation over the southeastern United States and especially over Florida has a significant contribution from diurnal variability, which includes the sea breeze convection along the coastlines. We now analyze an individual sea breeze event from 12 August 1991 in FLAReS1.0. This particular event was studied by *Wakimoto and Atkins* [1994] over central Florida as part of the Convection and Precipitation/Electrification (CaPE) experiment. Figure 13 shows 10-m wind vectors, convergence, cloud cover, and precipitation at two-hour intervals from 1600 UTC to

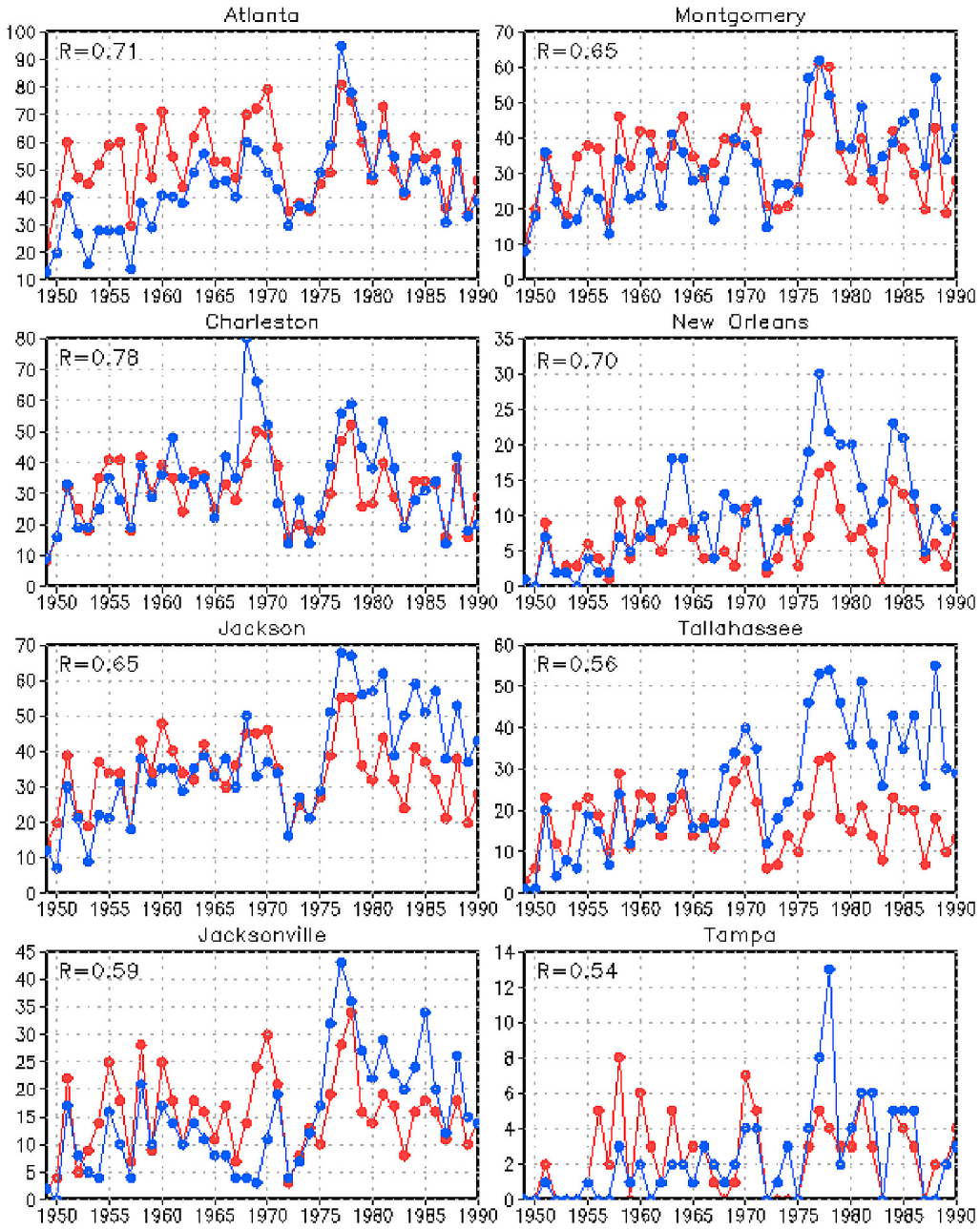

Figure 10. The number of days in which the minimum temperature drops below 0°C in each winter from 1948 to 49 through 1989–90 for several major cities from FLAReS1.0 (red) and station climatological observations (blue). The correlation coefficients between FLAReS1.0 and the station observations are shown at the top-left of each panel.

0000 UTC to monitor the progression of the event. At 1800 UTC (Figure 13a), a sea breeze is developing along the east coast in the presence of a weak to moderate southwesterly ambient flow. A large area of weak divergence is analyzed offshore. This is in agreement with the findings of *Stefanova et al.* [2012] in their studies with the CLARReS10 analysis. Meanwhile, a weaker area of convergence is seen developing in the Tampa Bay area. As the day progresses, the sea breeze front on the east coast does not move much, while the west coast sea breeze front propagates inland. Clouds and rain begin to develop at 2000 and 2200 UTC (Figures 13b and 13c), and by 0000 UTC (Figure 13d) a large portion of south-central Florida is covered in rain as the opposing sea breeze fronts begin to converge. This pattern is in agreement with the diurnal maximum plotted in Figure 6, and the relationship between the ambient wind and the sea breeze front propagation agrees with theory [*Blanchard and Lopez*, 1985]. The amount of precipitation coverage in FLAReS1.0 during this event is in reasonable agreement with observations from the CPC daily U.S. unified precipitation data set (not shown). The 10-km

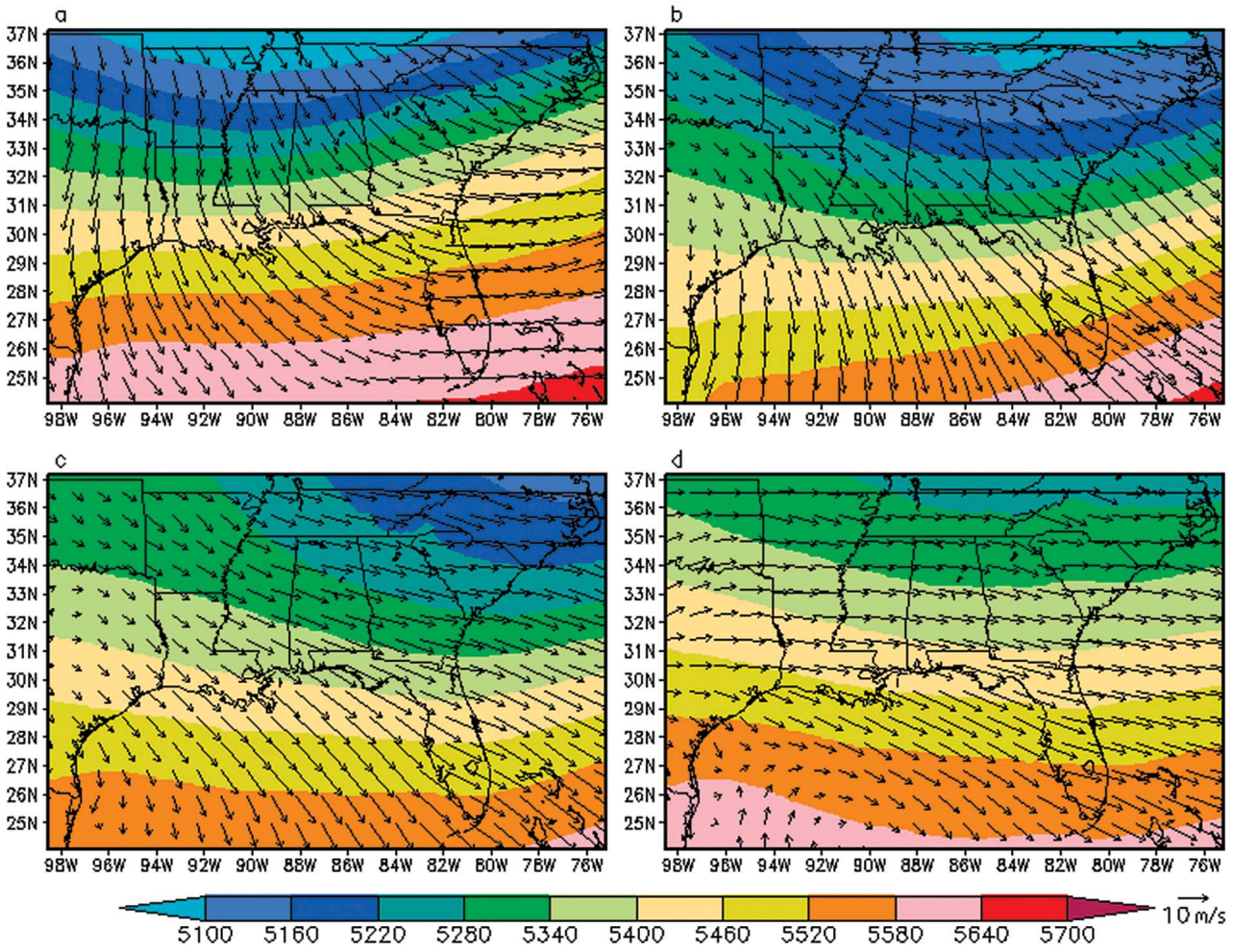

Figure 11. Daily average 500–1,000 mb thickness (m) overlaid with 850 mb wind vectors from FLAReS1.0 on (a) 20, (b) 21, (c) 22, and (d) 23 January 1985.

grid spacing of FLAReS1.0 does not resolve the microscale processes observed by *Wakimoto and Atkins* [1994] that lead to the formation of clouds and rainfall.

[18] Tropical cyclones provide another major source of precipitation in the southeastern United States. In addition, they are often high-impact events that result in catastrophic flooding and wind damage. To determine how accurately FLAReS1.0 portrays these systems, we analyze wind, sea level pressure, and precipitation data during the Labor Day Hurricane of 1935. The Labor Day Hurricane struck the Florida Keys late on 2 September 1935 as a category 5 storm before proceeding north along the west coast of the Florida peninsula and striking north Florida as a category 2 [*McDonald*, 1935]. FLAReS1.0 clearly shows a low pressure center and associated counterclockwise circulation that very closely match the actual track of the hurricane (Figures 14a–14d), but the intensity and structure of the storm are poorly reflected. The wind speeds and central pressure are greatly underestimated in FLAReS1.0, and the strongest winds are too far removed from the center. This is a common issue in climate simulations due to the low resolution of the climate models [*Manabe et al.*, 1970; *Bengtsson et al.*, 1982, 1995; *Tsutsui and Kasahara*, 1996]. In FLAReS1.0 although the spatial resolution at 10 km is greatly improved compared to the global climate models, it is limited by the coarse boundary conditions of the 20CR, which fails to resolve minimum pressure and maximum winds near the eyewall (not shown). FLAReS1.0 does however show a large shield of moderate to heavy rain associated with the hurricane with even some spiral banding features evident (Figures 14e–14h); this was also observed in the RSM simulation of another related study by *Camargo et al.* [2007]. The storm total precipitation in the model (not shown) is generally close to 100 mm over most of the Florida peninsula, with localized amounts exceeding 250 mm. Since these values are close to what is to be expected from a land-falling tropical cyclone, we can suggest from this case study that FLAReS1.0 could be further explored to understand the hydrologic impacts of tropical cyclones on the climate of the region. However, FLAReS1.0 does not capture the intensity or structure of individual storms.

[19] The final case study we analyze with FLAReS1.0 is the frontal system that impacted the southeastern United States on 13 March 1993. This storm was one of the most severe frontal systems to ever strike the region, and is often called the "storm of the century" or the "1993 superstorm." The system brought record-breaking snowfall to much of the East Coast and caused damaging winds and tornadoes in Florida [*Kocin et al.*, 1995]. We trace the evolution of this

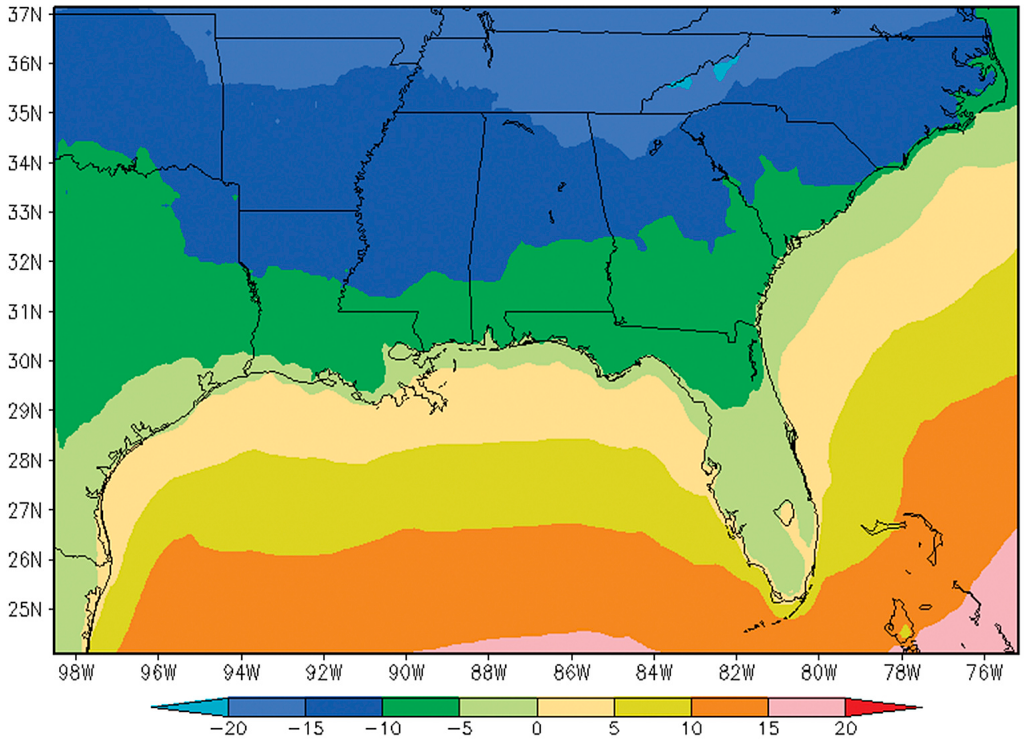

Figure 12. Minimum temperature (°C) recorded in FLAReS1.0 during the 4-day period from 20 Jan. 1985 through 23 Jan. 1985.

system back to 1200 UTC on 12 March, when it was a comparatively weak low off the Texas coast (Figures 15a and 15d). At this point, the pressure and precipitation fields in FLAReS1.0 are in strong agreement with the synoptic charts in the analysis by *Kocin et al.* [1995]. Twelve hours later, the system is deepening in the Gulf of Mexico, dropping to a minimum pressure of approximately 995 hPa (Figure 15b), but this is considerably weaker than the observed minimum pressure of 984 hPa at this time. By 1200 UTC on 13 March, the system has strengthened to a minimum pressure of 976 hPa near the Georgia-South Carolina border (Figures 15c and 15f). This is slightly weaker than the observed pressure of 972 hPa, but it is similar to the minimum pressure analyzed by CLARReS10-ERA40 [*Stefanova et al.*, 2012]. The precipitation field shows a classic comma shape, with a squall line near the east coast of Florida. This squall line actually moved across the state between 0400 and 0700 UTC, so the timing is a few hours late in the model. The model accurately generates snowfall reaching the Gulf Coast of Mississippi, Alabama, and extreme western Florida, as indicated by the location of the 0°C isotherm, with heavier snow falling in northern Georgia into the Carolinas. The storm total precipitation in the model (not shown) is 40–80 mm for most areas, with localized amounts exceeding 150 mm. These amounts are slightly higher than in CLARReS-ERA40 or the observations, but otherwise the effects of this storm are captured remarkably well by FLAReS1.0.

4. Discussion and Conclusions

[20] We have performed dynamical downscaling on the 20CR global reanalysis available on a 2° grid to a 10-km grid over the southeastern United States and the Gulf of Mexico to create the FLAReS1.0 data set. Despite the improved resolution, there are substantial biases in the precipitation climatology, especially in southern Florida and in the Carolinas. We determined that these biases are generally caused by increased precipitation frequency, particularly during the summer months. The biases are systematic and can easily be corrected to facilitate regional climate studies. The seasonal precipitation cycle is portrayed reasonably well in FLAReS1.0, with the spatial pattern closely matching the observations, although some localized biases exist in the magnitude of the seasonal peak. The climatological temperature data in FLAReS1.0 is generally within a 1–2°C of observations for all seasons of the year, and the seasonal cycle is portrayed extremely well.

[21] Our study of several phenomenological events reveals that the effects of frontal systems, tropical cyclones, and sea breezes on the local climate are well-represented in FLAReS1.0, but there are inaccuracies in the portrayal of individual events. In particular, the intensity of extreme weather events, such as frontal systems, Arctic outbreaks, and tropical cyclones tends to be underestimated. FLAReS1.0 does accurately portray the freeze climatology across the southeastern United States, but the severity of the most extreme cold events is underestimated. We believe that the simulation of the intensity and evolution of extreme weather events in FLAReS1.0 is limited somewhat by the forcing of the coarsely resolved 20CR global reanalysis and also by the errors of the RSM.

[22] The temporal length of the FLAReS1.0 data set makes it ideal for studying long-term variability, and the 10-km grid spacing allows for the resolution of mesoscale variations

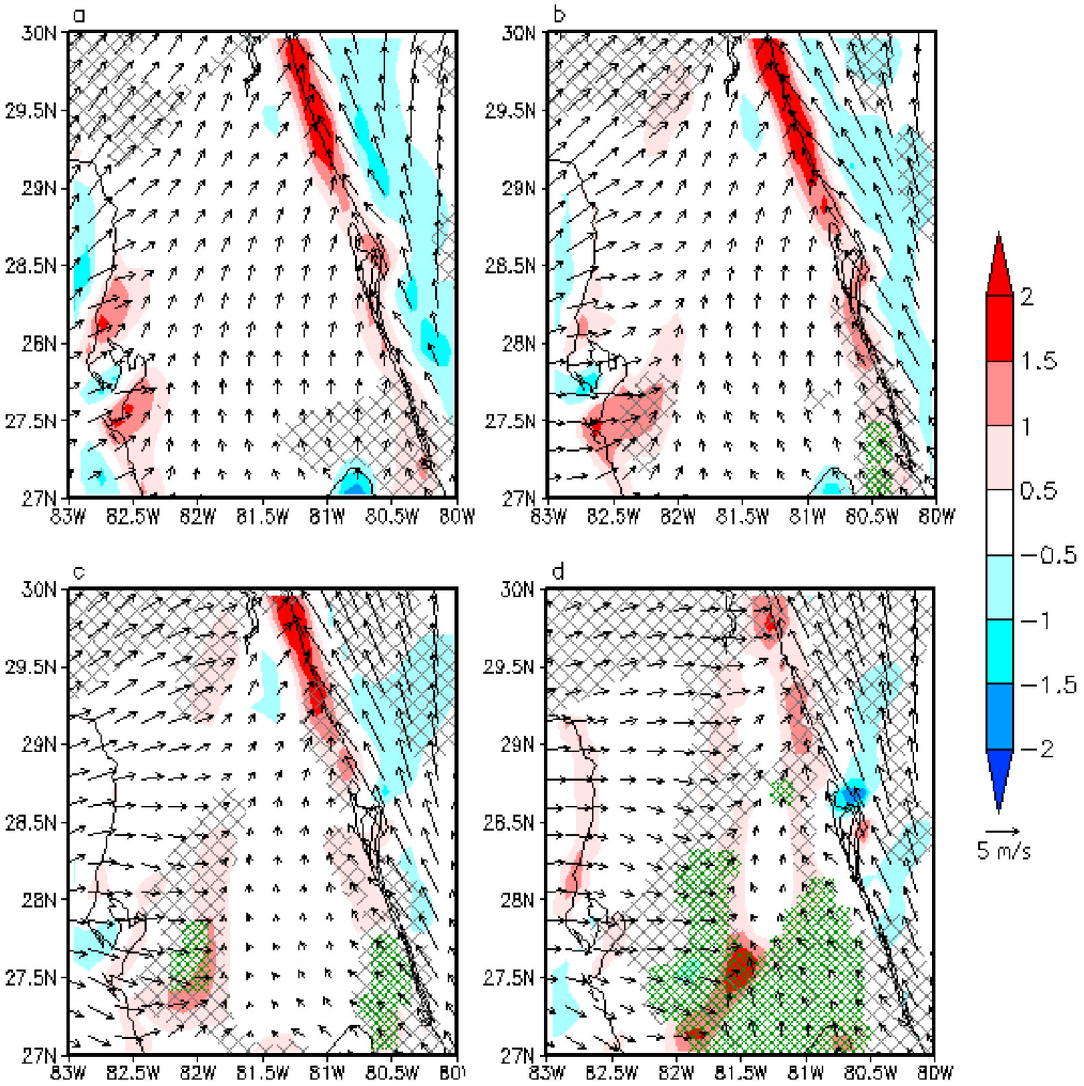

Figure 13. Surface wind vectors, convergence (shading; 10^{-4} s^{-1}), cloud cover (gray hatching), and precipitation (green hatching) at (a) 1800, (b) 2000, (c) 2200, and (d) 0000 UTC during the 12 August 1991 sea breeze event in central Florida.

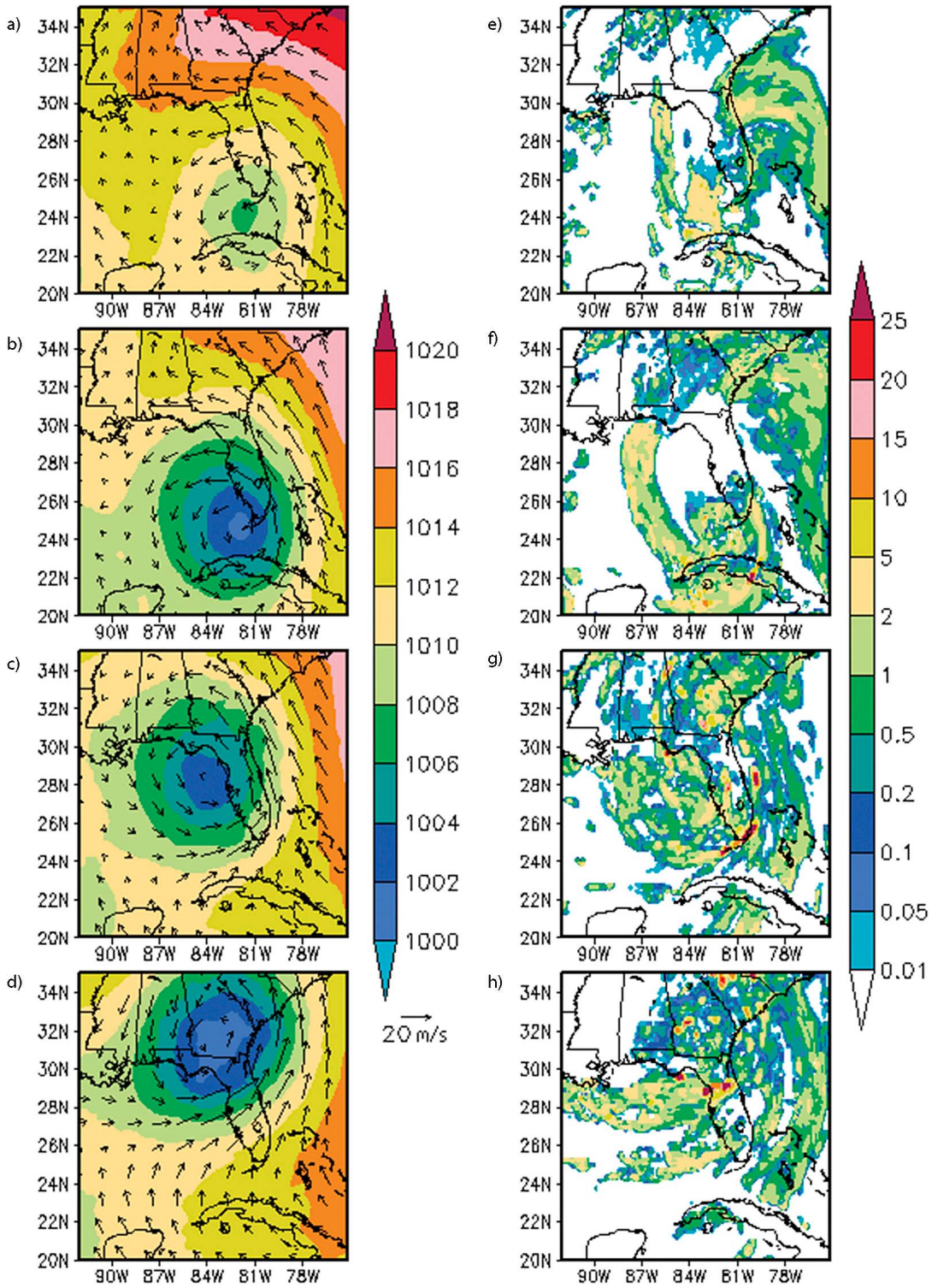

Figure 14. (a–d) Mean sea level pressure (hPa) overlaid with 925 mb wind vectors at 24-h intervals starting at 1200 UTC on 2 September 1935. (e–h) The same as Figures 14a–14d but showing hourly precipitation (mm).

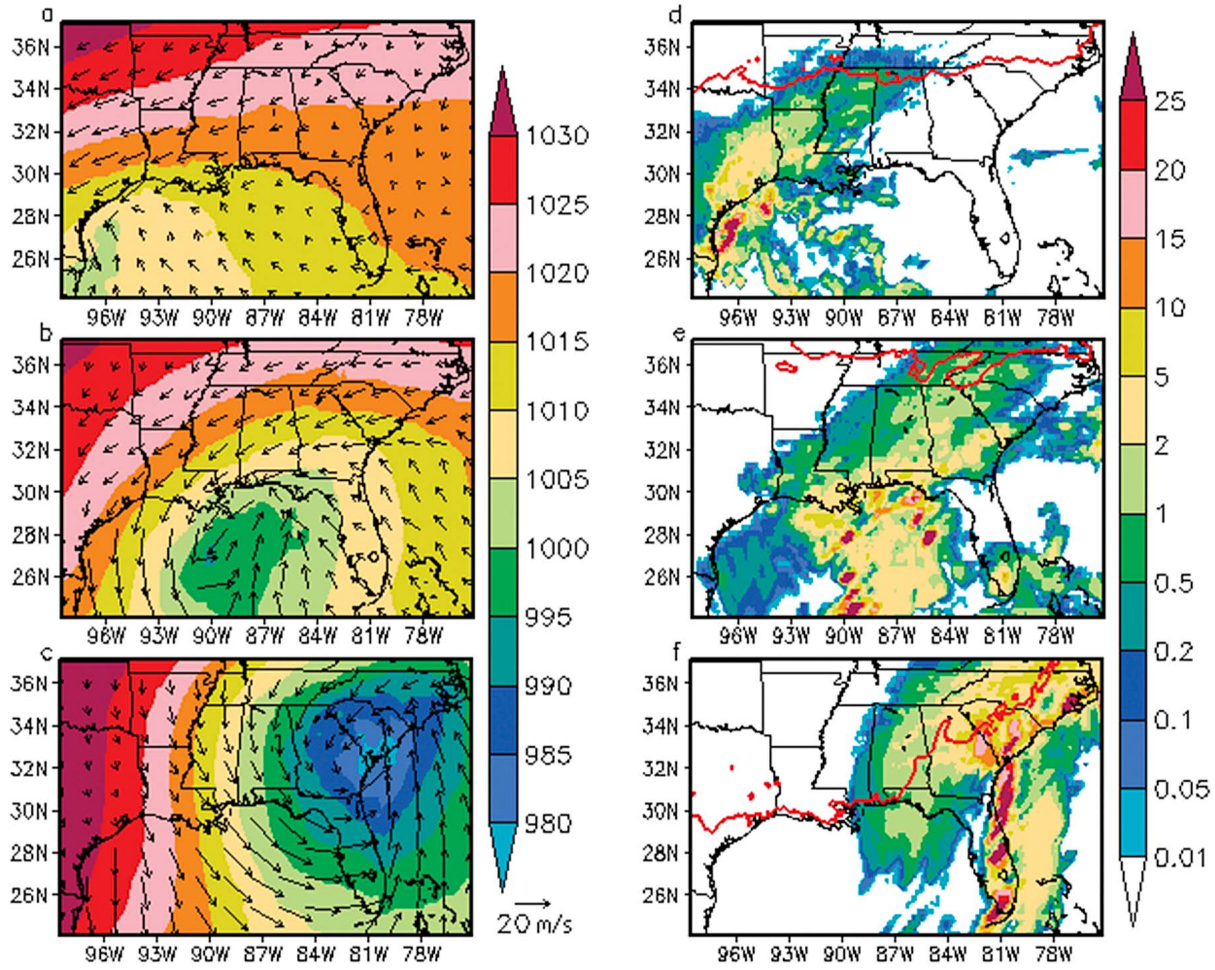

Figure 15. (a–c) Mean sea level pressure overlaid with surface wind vectors at 12-h intervals starting at 1200 UTC on 12 March 1993. (d–f) The same as Figures 15a–15c but showing hourly precipitation (mm; shaded) and the location of the 0°C isotherm (thick red line).

like the sea breeze circulations, frontal boundaries, and squall lines, which are all major components of the regional climate. We believe that the FLAReS1.0 downscaling data can be exploited further for application studies that require high resolution climate data to understand the impact of low frequency variations of climate in the southeastern United States.

[23] **Acknowledgments.** This work was supported by grants from NOAA (NA07OAR4310221), USGS (06HQGR0125), USDA (027865), and CDC (U01EH000421). Its contents are solely the responsibility of the authors and do not necessarily represent the official views of the acknowledged funding agencies.

References

Bengtsson, L., H. Böttger, and M. Kanamitsu (1982), Simulation of hurricane-type vortices in a general circulation model, *Tellus*, *34*, 440–457, doi:10.1111/j.2153-3490.1982.tb01833.x.

Bengtsson, L., M. Botzet, and M. Esch (1995), Hurricane-type vortices in a general circulation model, *Tellus, Ser. A*, *47*, 175–196.

Bengtsson, L., et al. (2007), The need for a dynamical climate reanalysis, *Bull. Am. Meteorol. Soc.*, *88*, 495–501, doi:10.1175/BAMS-88-4-495.

Blanchard, D. O., and R. E. Lopez (1985), Spatial patterns of convection in south Florida, *Mon. Weather Rev.*, *113*, 1282–1299, doi:10.1175/1520-0493(1985)113<1282:SPOCIS>2.0.CO;2.

Byers, H. R., and H. R. Rodebush (1948), Causes of thunderstorms of the Florida peninsula, *J. Meteorol.*, *5*, 275–280, doi:10.1175/1520-0469(1948)005<0275:COTOTF>2.0.CO;2.

Camargo, S. J., H. Li, and H. Sun (2007), Feasibility study for downscaling seasonal tropical cyclone activity using the NCEP regional spectral model, *Int. J. Climatol.*, *27*, 311–325, doi:10.1002/joc.1400.

Castro, C. L., R. A. Pielke Sr., and G. Leoncini (2005), Dynamical downscaling: Assessment of value retained and added using the regional atmospheric modeling system (RAMS), *J. Geophys. Res.*, *110*, D05108, doi:10.1029/2004JD004721.

Compo, G. P., et al. (2011), The Twentieth Century Reanalysis project, *Q. J. R. Meteorol. Soc.*, *137*, 1–28, doi:10.1002/qj.776.

Daly, C., R. P. Neilson, and D. L. Phillips (1994), A statistical-topographical model for mapping climatological precipitation over mountainous terrain, *J. Appl. Meteorol.*, *33*, 140–158, doi:10.1175/1520-0450(1994)033<0140:ASTMFM>2.0.CO;2.

Dee, D. P., et al. (2011), The ERA-Interim reanalysis: Configuration and performance of the data assimilation system, *Q. J. R. Meteorol. Soc.*, *137*, 553–597, doi:10.1002/qj.828.

Downton, M. W., and K. A. Miller (1993), The freeze risk to Florida citrus. Part II: Temperature variability and circulation patterns, *J. Clim.*, *6*, 364–372, doi:10.1175/1520-0442(1993)006<0364:TFRTFC>2.0.CO;2.

Ek, M. B., K. E. Mitchell, Y. Lin, E. Rogers, P. Grunmann, V. Koren, G. Gayno, and J. D. Tarpley (2003), Implementation of Noah land surface model advances in the National Centers for Environmental Prediction operational mesoscale Eta model, *J. Geophys. Res.*, *108*(D22), 8851, doi:10.1029/2002JD003296.

Higgins, R. W., J. E. Janowiak, and Y.-P. Yao (1996), A gridded hourly precipitation data base for the United States (1963–1993), report, 47 pp., Natl. Cent. for Environ. Predict., Camp Springs, Md.

Hong, S.-Y., and H. L. Pan (1998), Convective trigger function for a mass flux cumulus parameterization scheme, *Mon. Weather Rev.*, *126*, 2599–2620, doi:10.1175/1520-0493(1998)126<2599:CTFFAM>2.0.CO;2.

Juang, H. M. H., and M. Kanamitsu (1994), The NMC nested regional spectral model, *Mon. Weather Rev.*, *122*, 3–26, doi:10.1175/1520-0493(1994)122<0003:TNNRSM>2.0.CO;2.

Kalnay, E., et al. (1996), The NCEP/NCAR 40-year reanalysis project, *Bull. Am. Meteorol. Soc.*, *77*, 437–471, doi:10.1175/1520-0477(1996)077<0437:TNYRP>2.0.CO;2.

Kanamaru, H., and M. Kanamitsu (2007a), Scale-selective bias correction in a downscaling of global analysis using a regional model, *Mon. Weather Rev.*, *135*, 334–350, doi:10.1175/MWR3294.1.

Kanamaru, H., and M. Kanamitsu (2007b), Fifty-seven-year California reanalysis downscaling at 10 km (CaRD10). Part II: Comparison with North American regional analysis, *J. Clim.*, *20*, 5572–5592, doi:10.1175/2007JCLI1522.1.

Kanamitsu, M., and H. Kanamaru (2007), Fifty-seven-year California reanalysis downscaling at 10 km (CaRD10). Part I: System detail and validation with observations, *J. Clim.*, *20*, 5553–5571, doi:10.1175/2007JCLI1482.1.

Kanamitsu, M., W. Ebusuzaki, J. Woollen, S.-K. Yang, J. Hnilo, M. Fiorino, and G. L. Potter (2002), NCEP-DOE AMIP-II reanalysis (R-2), *Bull. Am. Meteorol. Soc.*, *83*, 1631–1643, doi:10.1175/BAMS-83-11-1631.

Kanamitsu, M., K. Yoshimura, Y.-B. Yhang, and S.-Y. Hong (2010), Errors of interannual variability and multi-decadal trend in dynamical regional climate downscaling and its corrections, *J. Geophys. Res.*, *115*, D17115, doi:10.1029/2009JD013511.

Kocin, P. J., P. N. Schumacher, R. F. Morales Jr., and L. W. Uccellini (1995), Overview of the 12–14 March 1993 superstorm, *Bull. Am. Meteorol. Soc.*, *76*, 165–182, doi:10.1175/1520-0477(1995)076<0165:OOTMS>2.0.CO;2.

Lin, Y., and K. E. Mitchell (2005), The NCEP stage II/IV hourly precipitation analyses: Development and applications, paper presented at 19th Conference on Hydrology, Am. Meteorol. Soc., San Diego, Calif.

Manabe, S., J. L. Holloway, and H. M. Stone (1970), Tropical circulation in a time-integration of a global model of the atmosphere, *J. Atmos. Sci.*, *27*, 580–613, doi:10.1175/1520-0469(1970)027<0580:TCIATI>2.0.CO;2.

McDonald, W. F. (1935), The hurricane of August 31 to September 6, 1935, *Mon. Weather Rev.*, *63*, 269–271, doi:10.1175/1520-0493(1935)63<269:THOATS>2.0.CO;2.

Mesinger, F., et al. (2006), North American regional reanalysis, *Bull. Am. Meteorol. Soc.*, *87*, 343–360, doi:10.1175/BAMS-87-3-343.

Miller, K. A. (1991), Response of Florida citrus growers to the freezes of the 1980's, *Clim. Res.*, *1*, 133–144, doi:10.3354/cr001133.

Miller, K. A., and M. W. Downton (1993), The freeze risk to Florida citrus. Part I: Investment decisions, *J. Clim.*, *6*, 354–363, doi:10.1175/1520-0442(1993)006<0354:TFRTFC>2.0.CO;2.

Misra, V., L. Moeller, L. Stefanova, S. Chan, J. J. O'Brien, T. J. Smith III, and N. Plant (2011), The influence of the Atlantic warm pool on the Florida panhandle sea breeze, *J. Geophys. Res.*, *116*, D00Q06, doi:10.1029/2010JD015367.

Mitchell, T. D., and P. D. Jones (2005), An improved method of constructing a database of monthly climate observations and associated high resolution grids, *Int. J. Climatol.*, *25*, 693–712, doi:10.1002/joc.1181.

Onogi, K., et al. (2007), The JRA-25 Reanalysis, *J. Meteorol. Soc. Jpn.*, *85*, 369–432, doi:10.2151/jmsj.85.369.

Rayner, N. A., D. E. Parker, E. B. Horton, C. K. Folland, L. V. Alexander, D. P. Rowell, E. C. Kent, and A. Kaplan (2003), Global reanalysis of sea surface temperature, sea ice, and night marine air temperature since the late nineteenth century, *J. Geophys. Res.*, *108*(D14), 4407, doi:10.1029/2002JD002670.

Rienecker, M. M., et al. (2011), MERRA: NASA's Modern-Era Retrospective Analysis for Research and Applications, *J. Clim.*, *24*, 3624–3648, doi:10.1175/JCLI-D-11-00015.1.

Saha, S., et al. (2010), The NCEP climate forecast system reanalysis, *Bull. Am. Meteorol. Soc.*, *91*, 1015–1057, doi:10.1175/2010BAMS3001.1.

Slingo, J. M. (1987), The development and verification of a cloud prediction scheme for the ECMWF model, *Q. J. R. Meteorol. Soc.*, *113*, 899–927, doi:10.1256/smsqj.47708.

Stefanova, L., V. Misra, S. Chan, M. Griffin, J. J. O'Brien, and T. J. Smith III (2012), A proxy for high-resolution regional reanalysis for the southeast United States: Assessment of precipitation variability in dynamically downscaled reanalyses, *Clim. Dyn.*, *38*, 2449–2466, doi:10.1007/s00382-011-1230-y.

Tiedtke, M. (1983), The sensitivity of the time-mean large-scale flow to cumulus convection in the ECMWF model, paper presented at Workshop on Convection in Large-Scale Models, Eur. Cent. for Medium-Range Weather Forecasts, Reading, U. K.

Tsutsui, J. I., and A. Kasahara (1996), Simulated tropical cyclones using the National Center for Atmospheric Research community climate model, *J. Geophys. Res.*, *101*(D10), 15,013–15,032, doi:10.1029/95JD03774.

Uppala, S., et al. (2005), The ERA-40 re-analysis, *Q. J. R. Meteorol. Soc.*, *137*, 553–597.

von Storch, H., H. Langenberg, and F. Feser (2000), A spectral nudging technique for dynamical downscaling purposes, *Mon. Weather Rev.*, *128*, 3664–3673, doi:10.1175/1520-0493(2000)128<3664:ASNTFD>2.0.CO;2.

Wakimoto, R. M., and N. T. Atkins (1994), Observations of the sea-breeze front during CaPE. Part I: Single-Doppler, satellite and cloud photogrammetry analysis, *Mon. Weather Rev.*, *122*, 1092–1114, doi:10.1175/1520-0493(1994)122<1092:OOTSBF>2.0.CO;2.